A novel multifunctional SERS microfluidic sensor based on ZnO/Ag nanoflower arrays for label-free ultrasensitive detection of bacteria

*Yue Liu, Guanwen Su, Wei Wang, Hongyuan Wei and Leping Dang,**

School of Chemical Engineering and Technology, Tianjin University, Tianjin 300072, People's Republic of China

*Corresponding author E-mail: dangleping@tju.edu.cn

1. Morphology Control of ZnO Nanoarrays

1.1 The influence of precursor solution concentration

Generally speaking, the concentration of precursors determines the grain size of the seed layer seeds, thereby determining the density of the nanowire array. The SEM images of ZnO nanoarrays prepared under different concentrations of precursor solutions, namely zinc acetate/ethanol solutions, are shown in Figure S1. From the graph, it can be seen that when the precursor concentration is 0.005 mol/L, only rod-shaped ZnO is generated, and no ZnO nanoarray is generated; When the current concentration of the precursor increases to 0.015 mol/L, dense cluster like ZnO aggregates begin to form, and no ZnO nanoarrays are formed; When the current drive concentration reaches 0.025 mol/L, the formation of ZnO nanoarrays and clustered ZnO aggregates begins to be observed; When the current drive concentration continues to increase to 0.05 mol/L, the number of clustered ZnO decreases while generating ZnO nanoarrays. When the precursor concentration is 0.005 mol/L, the low concentration prevents the formation of a continuous ZnO seed layer and instead separates ZnO crystal nuclei, making it impossible for ZnO to grow vertically; As the precursor concentration increases, the ZnO seed layer becomes more uniform, and at appropriate concentrations, dense vertically grown ZnO nanowire arrays will be generated. When the current

drive concentration is too high, the seed layer will overlap, and after exceeding a certain thickness, the sensitivity of nanowire density decreases, resulting in the formation of clustered ZnO aggregates. In the precursor concentrations of 0.025 mol/L and 0.05 mol/L for the generation of ZnO nanoarrays, the optimal conditions were selected as the 0.05 mol/L precursor solution with less clustered ZnO generation and more uniform vertical growth of ZnO nanoarrays.

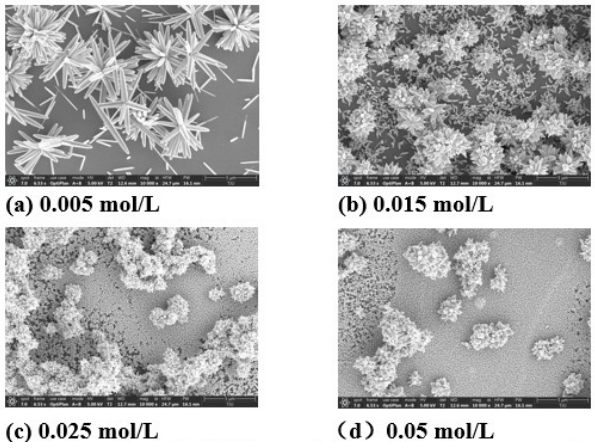

Fig. S1. SEM images of ZnO nanoarrays at different precursor concentrations.

1.2 The influence of the molar ratio of hexamethylenetetramine to zinc nitrate

The proportion of growth solution has a significant impact on the growth process of ZnO nanoarrays. By changing the molar ratio of HTMA and zinc nitrate in the growth solution, the SEM image of the ZnO nanoarray obtained is shown in Figure S2. From the figure, it can be seen that the change in the molar ratio of

HTMA and zinc nitrate has a significant impact on the morphology of ZnO nanoarrays. It is difficult to generate a complete ZnO nanoarray if the molar ratio of both is too high or too low. When the molar ratio of HTMA to zinc nitrate is 2:1, due to HTMA being a weak base, the concentration of [OH] - is higher, which accelerates the precipitation rate of ZnO and cannot maintain vertical growth, only rod-shaped ZnO is generated; When the molar ratio is 1:1 and 1:2, a dense layer of ZnO nanoarrays and clustered ZnO are generated; When the molar ratio reaches 1:4 and 1:6, excessive amounts of "Zn" ^ "2+" may lead to the direct nucleation of "Zn" ^ "2+" in the solution and the generation of cluster shaped ZnO and rod shaped ZnO, which cannot generate vertically grown ZnO nanoarrays. The comparison shows that when the molar ratio of HTMA and zinc nitrate is 1:1, the ZnO nanowire array is uniform and dense, providing more "hotspots". Therefore, a molar ratio of HTMA and zinc nitrate of 1:1 is chosen as the most suitable preparation condition.

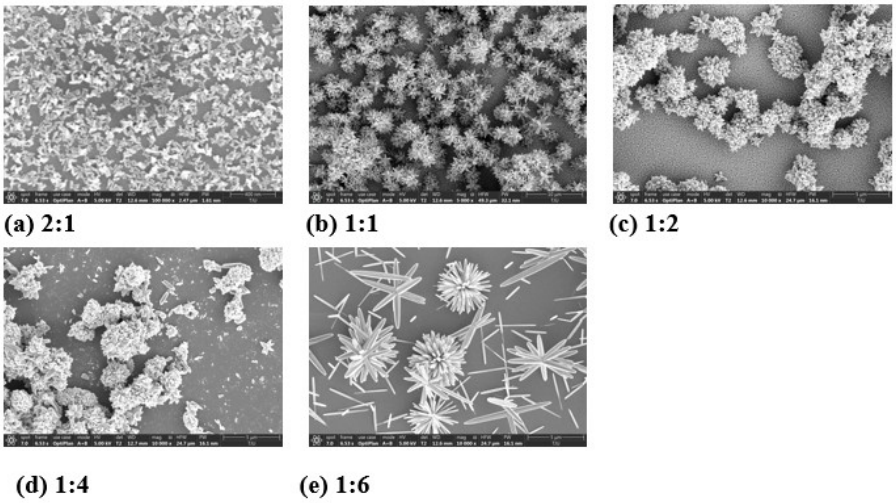

Fig. S2. SEM images of ZnO nanoarrays under different HTMA and zinc nitrate molar ratios.

1.3 The influence of polyethylene imine addition amount

The SEM images of ZnO nanoarrays prepared with different amounts of polyethyleneimine added in the growth solution are shown in Figure S3. From the figure, it can be seen that without the addition of polyethyleneimine in the growth solution, the generated ZnO nanoarrays and cluster shaped ZnO are very dense and unevenly distributed. This is because the combination of polyethyleneimine and ammonia can prevent nucleation and precipitation. Without the addition of polyethyleneimine, the growth direction of ZnO is not controllable, resulting in very uneven finished products. As the concentration of polyethyleneimine in the solution increases, the density of the generated ZnO nanoarrays increases, and the diameter distribution becomes uniform, and the defects in the nanorods decrease.

This is because polyethyleneimine can adsorb on the side surface of the generated ZnO nanowires through electrostatic action to reduce the radial growth rate of ZnO, promote the vertical growth of ZnO nanowires, and improve their aspect ratio, thereby obtaining vertically grown, tightly and uniformly arranged ZnO nanoarrays. After comparison, 0.20 mL of polyethyleneimine was selected as the most suitable condition for cluster like ZnO with less generation and relatively uniform and dense ZnO nanowire arrays.

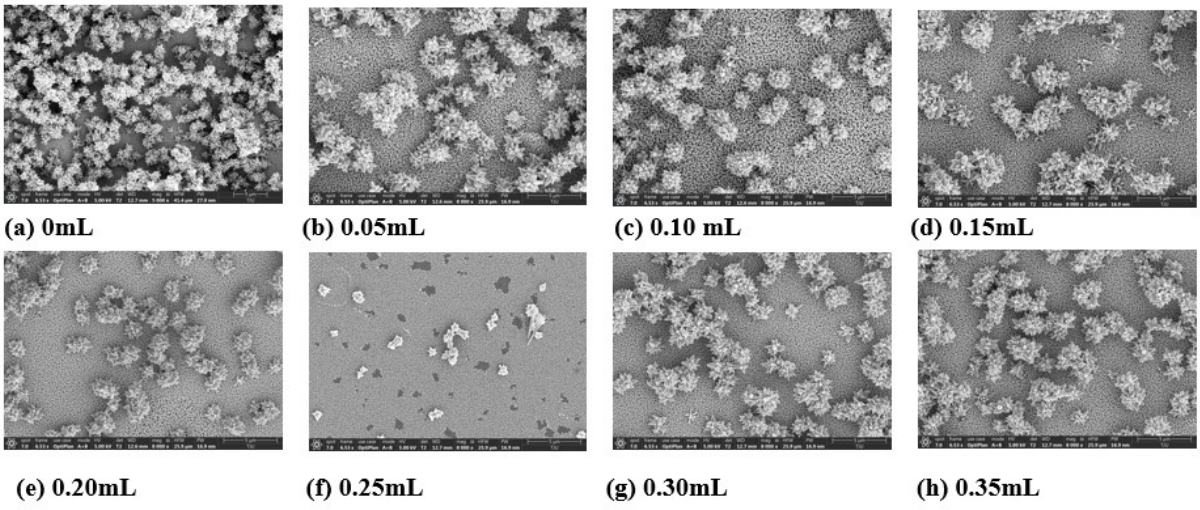

Fig. S3. SEM images of ZnO nanoarrays with different amounts of polyethyleneimine added.

1.4 The influence of reaction time

As the reaction time changes, the SEM characterization results of ZnO nanoarrays are shown in Figure S4. From the graph, it can be seen that with the increase of reaction time, the growth status of ZnO nanoarrays does not have a

clear regularity, and there is no growth pattern of gradually dense or sparse arrays as time increases. Clustered ZnO growing on the nanoarrays will gradually become dense with the increase of reaction time. The length of reaction time indicates the degree of chemical reaction. As the chemical reaction proceeds, ZnO nanowire arrays are first grown on the seed layer. After the ZnO nanowire layer reaches a certain thickness, ZnO continues to precipitate, but no longer vertically forms nanowires, but instead clusters of ZnO aggregates are formed. The longer the chemical reaction takes, the more densely clustered ZnO is generated. Compared to others, the speed of hydrothermal deposition reaction is not slow. In this experiment, the most suitable reaction time condition was chosen to be 200 minutes with a denser ZnO nanoarray.

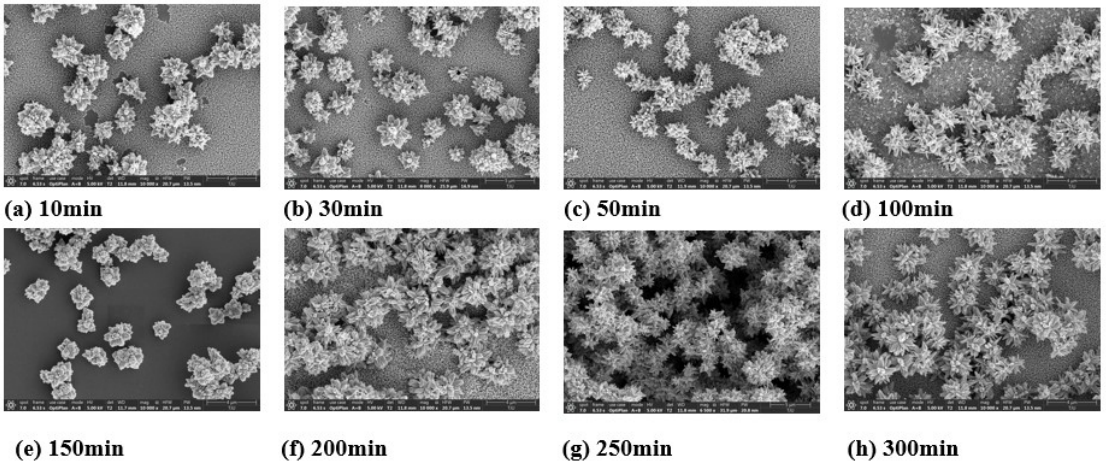

Fig. S4. SEM image of the morphology of ZnO nanoarrays as a function of reaction time.

2. The fabrication process of microfluidic SERS chips

This study used silicon wafers as the substrate material for SERS chips and prepared silver nanoparticle modified ZnO nanoflower arrays on the surface of the wafers using hydrothermal method. Subsequently, the prepared SERS chip is assembled into a customized microfluidic platform. The sample solution was transported to the microfluidic sensor through a peristaltic pump, and the interception, enrichment, and optical identification of pathogens in the microfluidic chip were successfully achieved using the microfluidic chip. This research achievement provides an effective method for the capture, enrichment, and optical detection of pathogens in clinical samples.

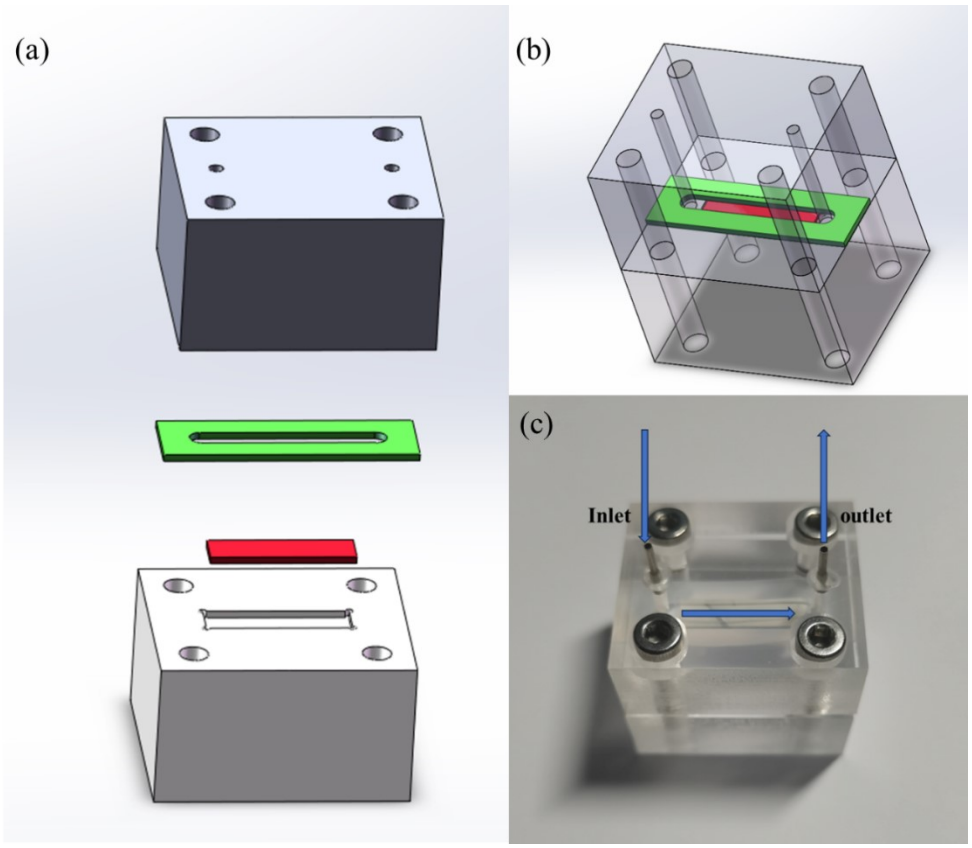

Fig. S5. (a) Schematic diagram of multi-layer structure (b) Schematic diagram of microfluidic chip (c) Physical diagram.

3. Supplementary data

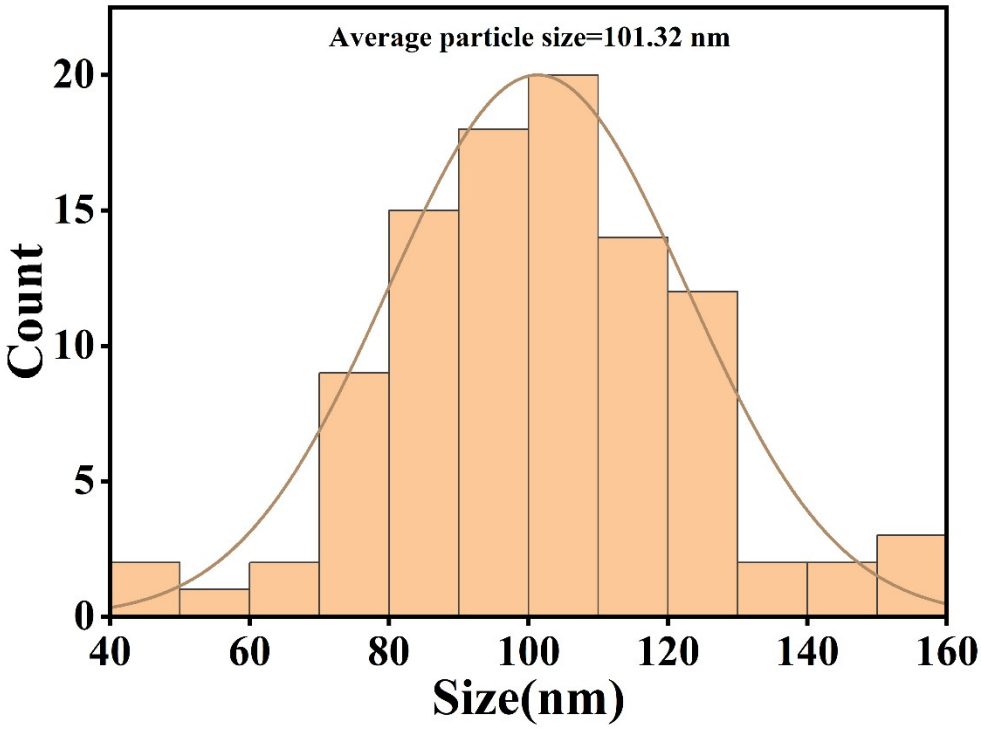

Fig. S6. Particle size distribution of Ag nanoparticles.

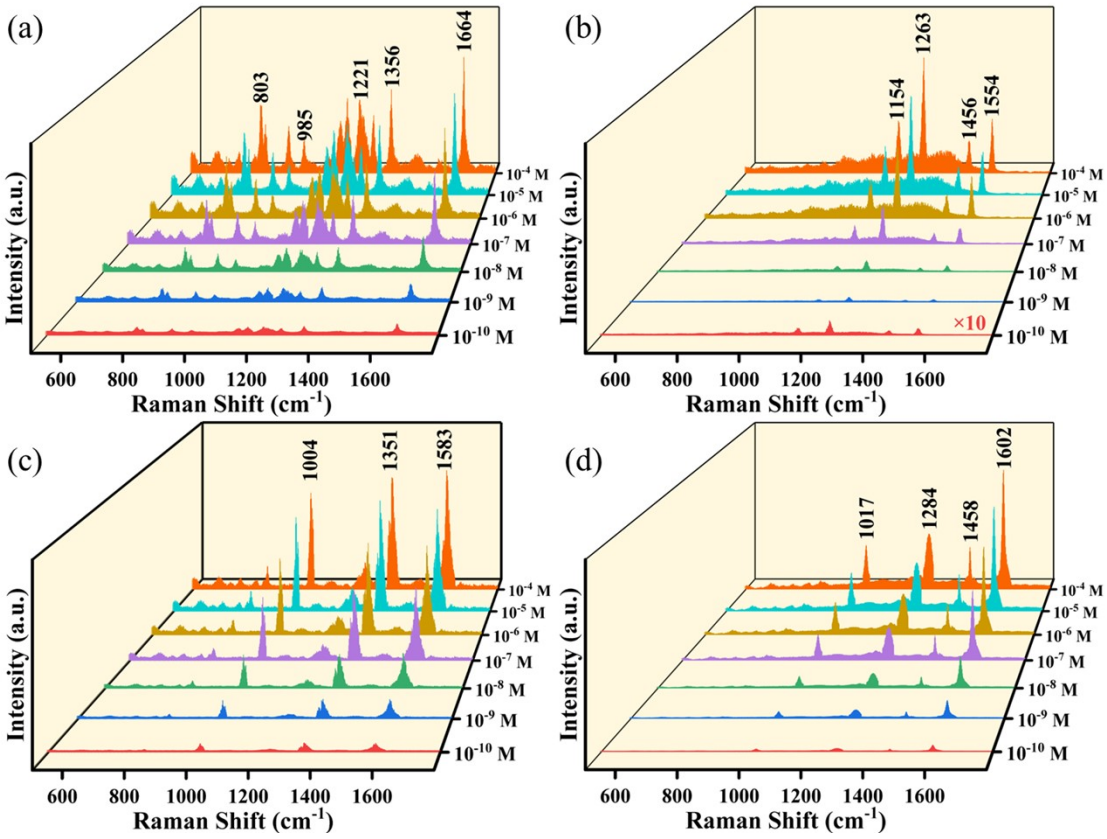

Fig. S7. Raman spectra of (a) malachite green, (b) chlorpyrifos, (c) cyhalothrin, and (d) thiabendazole at different concentrations.

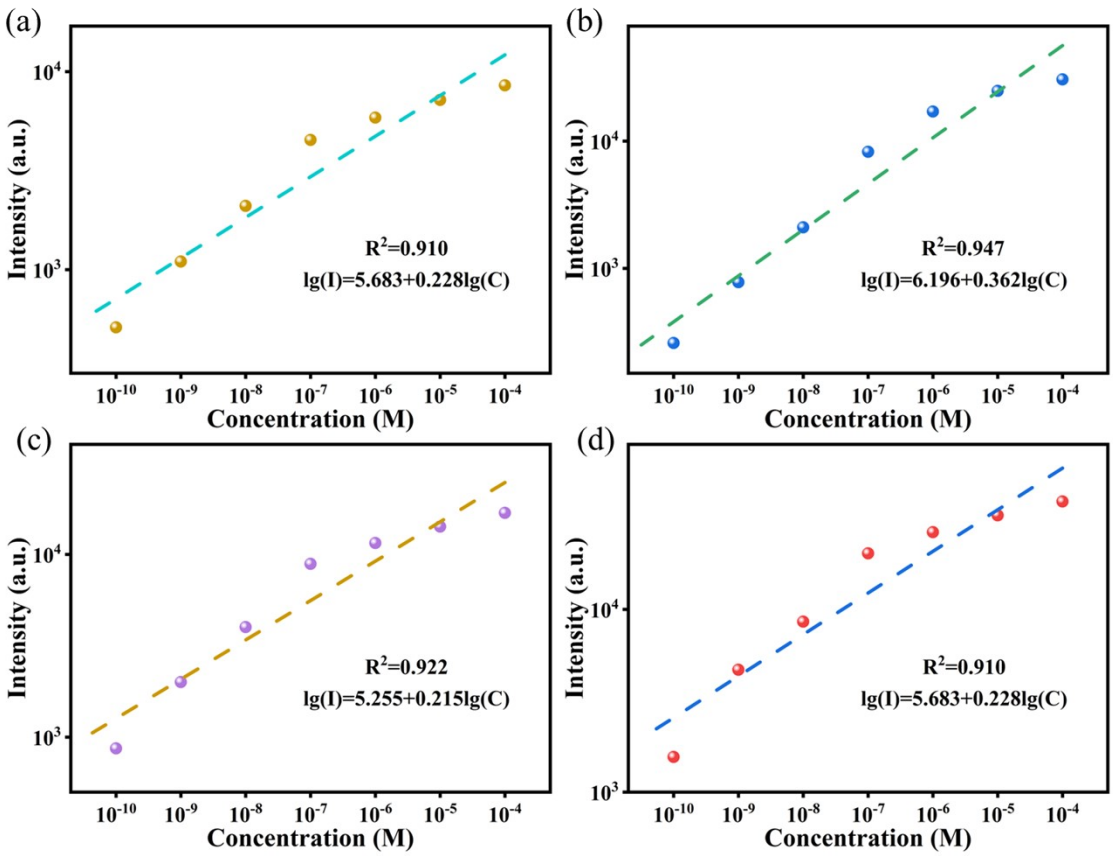

Fig. S8. The quantitative analysis diagram of (a) malachite green, (b) chlorpyrifos, (c) cyhalothrin, and (d) thiabendazole.

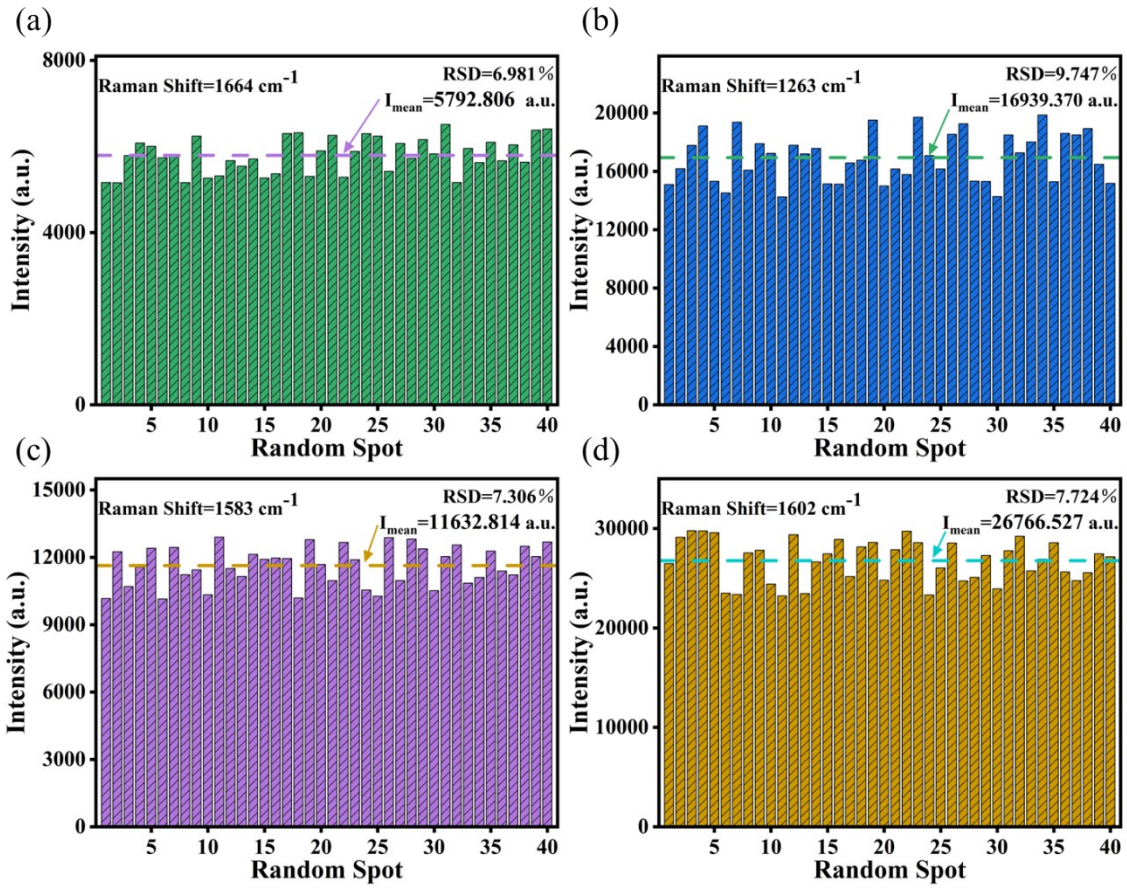

Fig. S9. The signal recurrence diagram of (a) malachite green, (b) chlorpyrifos, (c) cyhalothrin, and (d) thiabendazole.

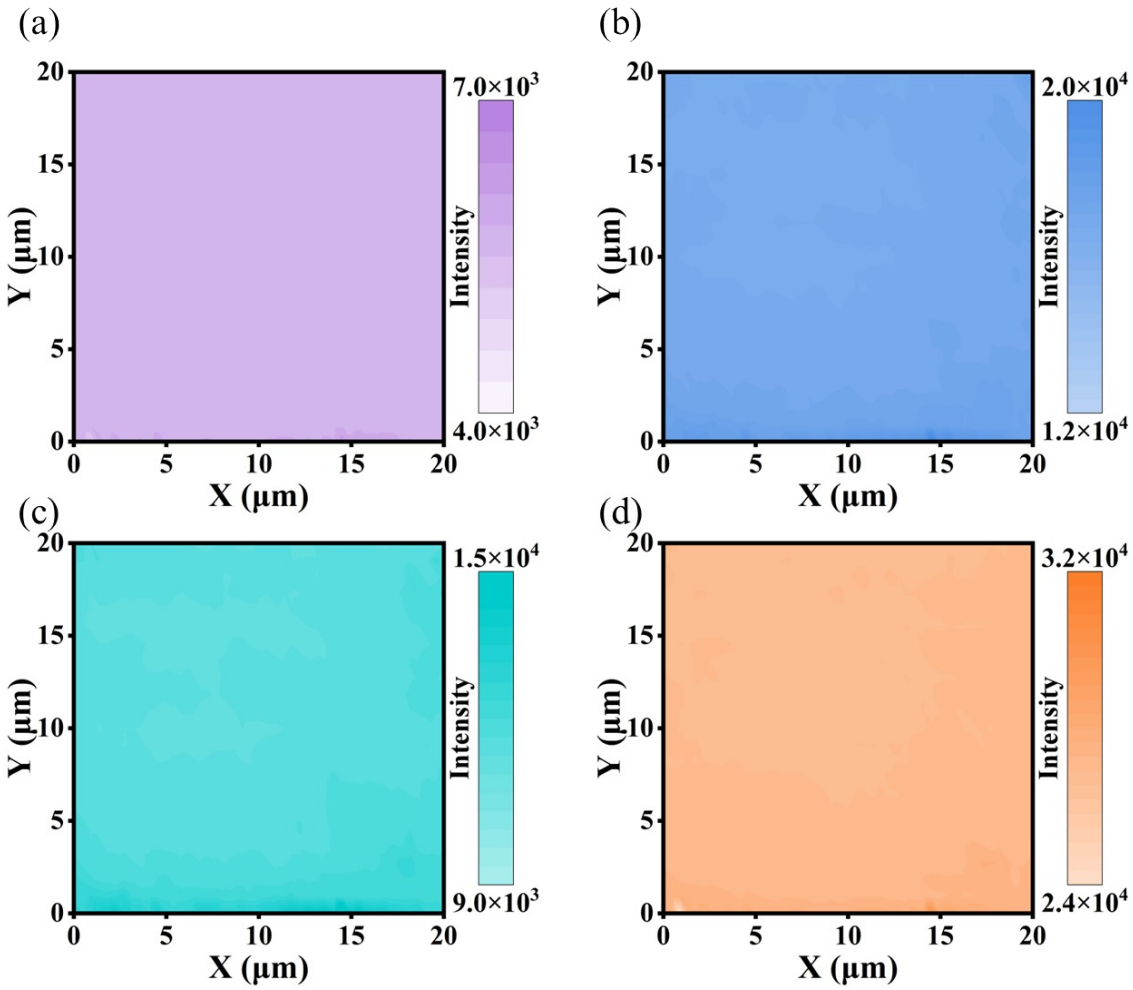

Fig. S10. The uniformity diagram of (a) malachite green, (b) chlorpyrifos, (c) cyhalothrin, and (d) thiabendazole.

4. Comparison of the Microfluidic SERS chip with other SERS substrates

Table S1. Comparison of the Microfluidic SERS chip with other SERS substrates.

SERS substrate	Target bacteria	LOD (CFU/mL)	Ref
SiO_2@Au/Ag	S. aureus	10^3	[1]
Ag–Cu_xO Nanostructures	E. subtilis, E. coli, E. faecalis, S. aureus, and S. mutans	10^3	[2]
Fe_3O_4@Au@PEI	E. coli and S. aureus	10^3	[3]
Cu/AgNP	S. aureus, and V. parahaemolyticus	10^4	[4]
AgNP	E. coli and S. epidermidis	$2.5*10^2$	[5]
Microfluidic SERS chip	E. coli, S. aureus, B. subtilis, and E. faecalis	10^2	This work

References

1. M. Wan, H. Zhao, L. Peng, X. Zou, Y. Zhao and L. Sun, *Polymers*, 2020, **12**.
2. F. Sahin, A. Camdal, G. Demirel Sahin, A. Ceylan, M. Ruzi and M. S. Onses, *ACS Applied Materials & Interfaces*, 2023, **15**, 11563-11574.
3. C. Wang, J. Wang, M. Li, X. Qu, K. Zhang, Z. Rong, R. Xiao and S. Wang, *The Analyst*, 2016, **141**, 6226-6238.
4. A. B. Beyene, W.-N. Su, H.-C. Tsai, W. A. Tegegne, C.-H. Chen, C.-C. Huang, D. Mares, V. Prajzler, W.-H. Huang and B. J. Hwang, *ACS Applied Nano Materials*, 2022, **5**, 11567-11576.
5. H. Zhou, D. Yang, N. P. Ivleva, N. E. Mircescu, R. Niessner and C. Haisch, *Analytical Chemistry*, 2014, **86**, 1525-1533.